



Chemical Interactions Between Aluminosilicate Base Sealants and the Components on the Anode Side of Solid Oxide Fuel Cells

N. Lahl, D. Bahadur,^a K. Singh, L. Singheiser, and K. Hilpert^z

Institute for Materials and Processing in Energy Systems, Forschungszentrum Jülich GmbH,
D-52425 Jülich, Germany

The chemical interactions between several aluminosilicate glasses and components at the anode side of SOFC have been investigated. Severe reactions occur if the modifier ions are Ba and Ca. MgO base sealants have been investigated in detail. The formation of some detrimental phases are seen. Cordierite forms with many reaction mixtures of sealants with ZrO₂ stabilized with 8 mol % Y₂O₃ (as electrolyte) or nickel (as anode). On the other hand, with oxide dispersion strengthened Cr₅Fe₁Y₂O₃ and steel, another detrimental phase, cristobalite, is favored. There appears to be a competitive formation of these two detrimental phases in some cases. In some of the interactions none of the detrimental phases appears. The diffusion behavior of the cations across the interfaces has been investigated. Among all the cations, chromium diffuses the maximum. The diffusion coefficient of chromium for the diffusion couples of different sealants with ODS alloy have been determined.

© 2002 The Electrochemical Society. [DOI: 10.1149/1.1467945] All rights reserved.

Manuscript submitted July 23, 2001; revised manuscript received November 26, 2001. Available electronically March 29, 2002.

The development of a suitable sealant is still an important demand for planar solid oxide fuel cell (SOFC) systems consisting of cell stacks because of the stringent requirements such as gas tightness, insulating properties, matching thermal expansion coefficients, good soldering behavior, and the chemical stability in both the oxidizing and reducing atmospheres.¹⁻³ The sealant, being in contact with all other components of planar SOFCs, is prone to degradation due to chemical interaction at the interfaces of these individual components and subsequent structural modifications. Literature on this aspect of interaction is rather limited.⁴⁻⁶ Several glass and glass ceramics have been studied as candidate materials for sealants. We have recently investigated many aluminosilicate glasses as potential sealant in the system AO-SiO₂-Al₂O₃-B₂O₃-N (A = Ba, Ca, and Mg; N = nucleating agents).⁷ By detailed differential thermal analysis (DTA), X-ray diffraction (XRD), thermal expansion, and electron microscopy work, we have determined the important characteristics of these glasses and their crystallization kinetics.^{7,8}

The chemical interactions of selected sealants with other materials of SOFC components at the anode side were investigated here. These materials are (i) ZrO₂ stabilized with 8 mol % Y₂O₃ (8YSZ) for the anode and the electrolyte, (ii) Ni for the anode, and (iii) oxide dispersion strengthened (ODS) Cr₅Fe₁Y₂O₃ alloy as well as the steel Fe18Cr1Al (DIN 1.4742) for the interconnect. LaCrO₃-based perovskites used as ceramic interconnect are not considered in this study. There is a general trend to use metallic interconnects in planar SOFC systems. The sealants were selected in order to elucidate the influence of varying alkaline earth metal ions as well as varying content of alumina and of TiO₂.

The rationale behind the choice of the specific aluminosilicate systems investigated and the specific issues addressed are described in the following. The different alkaline earth metals used, Ba, Ca, and Mg, act as modifiers and have widely different chemical properties such as field strength, ionic radius, and electronegativity. These properties have strong influence on the thermal expansion coefficient as well as the reactivity. Our objective was to investigate this influence. TiO₂ is generally used as a nucleating agent in aluminosilicate glasses. TiO₂ is known to induce phase separation in glasses and hence influences significantly crystallization kinetics and phase formation at the interfaces. We have intentionally varied the TiO₂ content to see its influence on the above-mentioned behavior. The investigation of the kinetics and the products of the reac-

tions between the different sealant compositions and the SOFC components is the task of this paper. Many of these reaction products could be detrimental for SOFCs. Hence, it is necessary to look for the conditions which inhibit or avoid the formation of detrimental phases. Moreover, interdiffusion has to be investigated. The most mobile species have to be identified and their diffusion coefficients determined. Measures to reduce diffusion are of interest.

Experimental

The glass compositions considered here together with their label are given in Table I. The details of the synthesis of glass and their characterization are given elsewhere.⁷ Grain sizes were not determined for each sealant composition. The typical size ranged between 1 and 20 μm. The chemical interactions between the sealants and the components of SOFC were investigated by annealing their powder mixtures under oxidizing and reducing conditions. Oxidizing conditions means annealing under ambient air. Reducing conditions were obtained by using initially a gas mixture composed of Ar with 4% H₂, which was humidified by passing over a water bath at 84°C and subsequently through a condenser at 56°C, leading to a H₂/H₂O ratio of 4. The grain size of the SOFC components in the powder mixtures amounted to <1 μm for 8YSZ, Ni, Cr₅Fe₁Y₂O₃, and Fe18Cr1Al. Diffusion couples were generally made by sandwiching a polished glass plate in between a polished interconnect alloy plate and a polished 8YSZ plate. In some cases the glass plate in the sandwich was replaced by a glass paste made of glass powder and an organic binder. The diffusion couple results by annealing the sandwich at temperatures above the glass transition temperature.

Phase analysis was conducted by XRD (Philips 1050, Eindhoven, Netherland; Cu Kα for all samples except sample MAST12 for which Co Kα radiation is used). The chemical composition of the phases were determined by scanning electron microscopy with energy-dispersive X-ray analysis, SEM/EDX (CAMSCAN/Tracor Northern, Middleton, WI) and transmission electron microscopy with EDX, TEM/EDX (Philips model CM 200 with GIF, energy filter, Eindhoven, Netherland). Using SEM/EDX, the diffusion profile of different cations was determined across the interfaces.

Results and Discussion

Table II shows the details of the phases identified by XRD, SEM/EDX, and TEM/EDX in the powder mixtures of the sealants with different components of SOFCs after annealing them at 1000°C for 1000 h under oxidizing and in part reducing conditions. The materials chosen were 8YSZ, Ni, ODS, and steel. The ASiO₃ (A = Ba, Ca, Mg) is a common product in most of the powder mixtures. Besides this, other phases are formed. Some of these phases are

^a Permanent address: Department of Metallurgical Engineering and Materials Science, Indian Institute of Technology Bombay, Mumbai-400076, India.

^z E-mail: k.hilpert@fz-juelich.de

Table I. Nominal composition of the glasses (in mol %) and their label.

Label	BaO	CaO	MgO	SiO ₂	Al ₂ O ₃	B ₂ O ₃	TiO ₂
BAS	45			45	5	5	
CAS		45		45	5	5	
MAS			45	45	5	5	
MAS10			40	45	10	5	
MAST10			38	45	10	5	2
MAST5			43	45	5	5	2
MAST12			35.6	43.1	12.8	3.6	4.9

known to be detrimental to SOFCs. The phase m-ZrO₂ is formed during the interaction of glass CAS with 8YSZ, which exhibits very high specific volume compared to stabilized zirconia.⁹ A further detrimental phase is cordierite (Mg₂Al₄Si₅O₁₈) formed in several interaction studies of MgO base glass with other components of SOFCs, in agreement with the phase diagram of the MgO-Al₂O₃-SiO₂ system. The thermal expansion coefficient (TEC) of this phase is very low ($2 \times 10^{-6}/\text{C}$) compared to that of other components of the fuel cell which is detrimental to SOFCs. The formation of another detrimental phase, cristobalite (SiO₂), occurs in many cases of interaction of the sealants with interconnect materials (ODS or steel). Cristobalite is known to undergo a structural transformation at 200°C involving a large volume change, which causes microcrack formation during cooling from the sealing tem-

perature. The nucleating agent TiO₂ was added to explore whether the growth of these undesirable phases can be suppressed by changing the crystallization kinetics.

Influence of alkaline earth metals on chemical interaction.—Figure 1 shows the typical SEM of interfaces of (a) BAS + ODS, (b) CAS + ODS, and (c) MAS + ODS heated at 1000°C under three different conditions. The first one is heated under reducing conditions for 1000 h, the second one under oxidizing conditions for 2 h, and the third one under oxidizing conditions for 1000 h. Though the experimental conditions are different, the results obtained for the interaction are generally valid for different sealants containing BaO, CaO, and MgO. The BaO and CaO base glasses show vigorous crystallization and reaction at the interface, whereas the MgO base glass exhibits very sober crystallization, and reaction. Similar results were obtained by experiments with powder mixtures. The crystallization kinetics of these glasses has already been studied by us earlier.⁷ Moreover, it has been shown that the CaO base glass in contact with 8YSZ gives rise to the formation of m-ZrO₂, which is detrimental to SOFC as mentioned previously. This is due to the diffusion of yttrium from 8YSZ into the glass. The detailed discussion of this interaction is given in an earlier paper from this laboratory.⁹ We have recently observed that the activation energy of crystallization increases significantly as we change the alkaline earth ion from Ba to Ca to Mg. This has been explained in terms of increasing field strengths of the alkaline earth ions.⁷ It has been observed that the diffusion couple of steel with the sealant BAS shows melting at the interface with detrimental corrosion attack of

Table II. Phases identified in powder mixtures of different sealants with SOFC components after their annealing at 1000°C over up to 1000 h in air or in reducing conditions (see Experimental section).^a

Sealant	Ni		YSZ		ODS		Steel
	Air	Red	Air	Red	Air	Red	Air
BAS	BaSiO ₃	BaSiO ₃	BaSiO ₃	BaAl ₂ Si ₂ O ₈	BaSi ₂ O ₅	BaSiO ₃	BaCrO ₄
	NiO	Ni	BaAl ₂ Si ₂ O ₈	Ba ₂ Zr ₂ Si ₃ O ₁₂	BaCrO ₄	Ba ₂ SiO ₄	Ba ₃ Fe ₃₂ O ₅₁
	BaAl ₂ Si ₂ O ₈	Ba ₂ Al ₂ O ₅ BaAl ₂ Si ₂ O ₈			Cr ₂ O ₃	Cr ₂ O ₃ BaAl ₂ Si ₂ O ₈	Ba ₂ Si ₃ O ₈
CAS	CaSiO ₃	CaSiO ₃	CaSiO ₃	CaSiO ₃	CaSiO ₃	CaSiO ₃	CaSiO ₃
	NiO	Ni	CaAl ₂ Si ₂ O ₈	Ca ₂ SiO ₄	Cr ₂ O ₃	Cr ₂ O ₃	Ca ₃ Cr ₂ (SiO ₄) ₃
		CaAl ₂ Si ₂ O ₈	Ca ₃ Zr(Si ₂ O ₉)O ₂	m-ZrO ₂	Ca ₃ Cr ₂ (SiO ₄) ₃	Ca ₃ Cr ₂ (SiO ₄) ₃	(Fe _{0.6} Cr _{0.4}) ₂ O ₃
MAS	Mg ₂ SiO ₄	Mg ₂ SiO ₄	Mg ₂ SiO ₄	Mg ₂ SiO ₄	(Mg,Fe) ₂ SiO ₄	Cr ₂ O ₃	
	NiO	Ni ^c	ZrSiO ₄	ZrSiO ₄	Spinel ^d	Spinel ^d	(Fe _{0.6} Cr _{0.4}) ₂ O ₃
MAS10	Mg ₂ SiO ₄	Mg ₂ SiO ₄	ZrSiO ₄	ZrSiO ₄	(Mg,Fe) ₂ SiO ₄	Spinel ^d	
	NiO	Ni	Mg ₂ SiO ₄	Mg ₂ SiO ₄	Spinel ^d	Cr ₂ O ₃	(Fe _{0.6} Cr _{0.4}) ₂ O ₃
					SiO ₂ ^e	SiO ₂ ^e	
MAST10	NiO	Ni	ZrSiO ₄	ZrSiO ₄	Mg ₂ TiO ₄	Spinel ^d	
		Mg ₂ SiO ₄	Mg ₂ SiO ₄		Spinel ^d	Cr ₂ O ₃	(Fe _{0.6} Cr _{0.4}) ₂ O ₃
MAST5	Mg ₂ SiO ₄	Mg ₂ SiO ₄	Mg ₂ SiO ₄	Mg ₂ SiO ₄	SiO ₂ ^e	SiO ₂ ^e	
	NiO	8YSZ	ZrSiO ₄	ZrO ₂ (cub)	Mg ₂ TiO ₄	Mg ₂ SiO ₄	
		ZrO ₂ (cub) ^b			Spinel ^d	Spinel ^d	(Fe _{0.6} Cr _{0.4}) ₂ O ₃
MAST12	Mg ₂ SiO ₄		Mg ₂ SiO ₄		SiO ₂ ^e	Cr ₂ O ₃	
	NiO		ZrSiO ₄		SiO ₂ ^e	SiO ₂ ^e	
	MgAl ₂ O ₄		ZrO ₂ (cub) ^b		(Mg,Fe) ₂ SiO ₄	SiO ₂ ^e	

^a The phases MgSiO₃ and Mg₂Al₄Si₅O₁₈ are present in the powder mixtures of MgO based sealants with other SOFC components unless otherwise specified.

^b No Mg₂Al₄Si₅O₁₈.

^c No MgSiO₃, no Mg₂Al₄Si₅O₁₈.

^d Means (Mg,Fe)(Cr,Al)₂O₄.

^e Represents cristobalite.

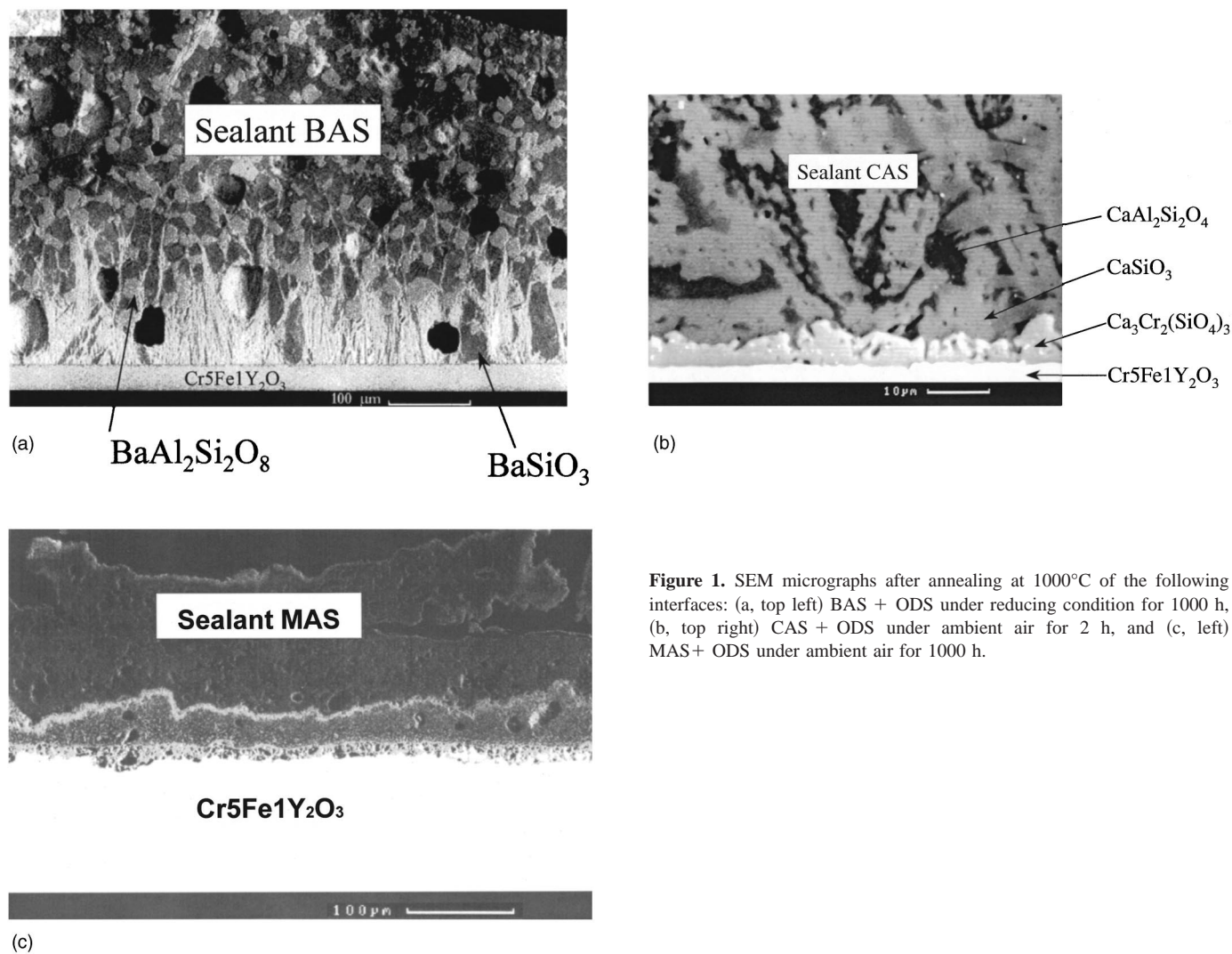


Figure 1. SEM micrographs after annealing at 1000°C of the following interfaces: (a, top left) BAS + ODS under reducing condition for 1000 h, (b, top right) CAS + ODS under ambient air for 2 h, and (c, left) MAS + ODS under ambient air for 1000 h.

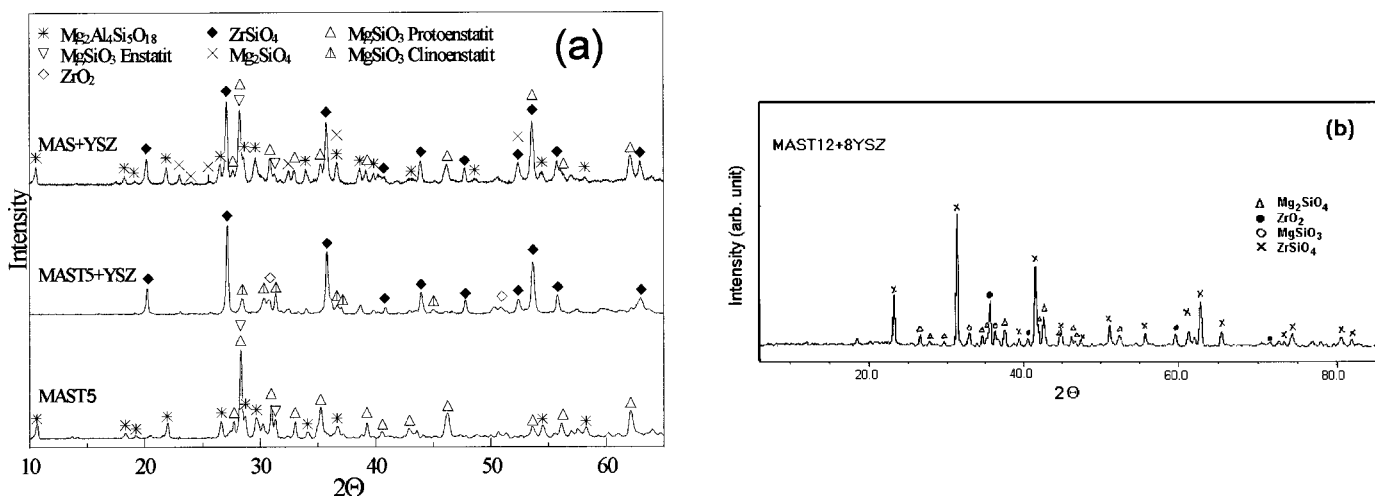


Figure 2. (a) XRD pattern of powder mixtures of MAS and MAST5 with 8YSZ heated at 1000°C for 500 h in air. The XRD pattern of sealant MAST5 is shown for comparison. (b) XRD pattern of powder mixture of MAST12 with 8YSZ under similar conditions as (a), with Co K α radiation.

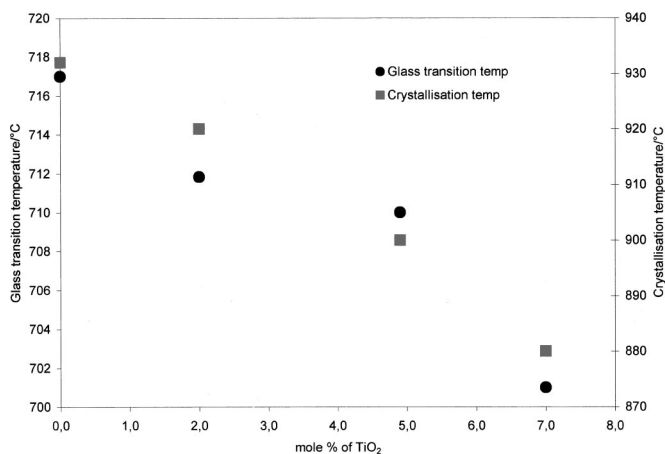


Figure 3. Variation of T_g and T_c (determined by DTA) with different mol % TiO_2 as nucleating agent in $\text{MgO-Al}_2\text{O}_3\text{-SiO}_2\text{-B}_2\text{O}_3$ glass composition.

the alloy after annealing at 1000°C for 1000 h under reducing conditions. FeO is possibly present under these conditions, forming mixtures with low eutectic temperatures. Severe interactions were also observed at the CAS/8YSZ interface leading to the diffusion of Ca into the 8YSZ.

In view of the low activation energy of crystallization of BaO and CaO base glasses and the extensive reaction of these glasses with other components of SOFCs, we have further carried out detailed investigations on MgO base glasses, which are now reported and discussed.

Chemical interactions of MgO base glasses.—Figure 2a shows the XRD pattern of powder mixtures of MAS and MAST5 with 8YSZ heated at 1000°C for 500 h in air. XRD data of the sealant MAST5 (heat-treated under similar conditions) is given for comparison. Figure 2b shows the XRD pattern of powder mixtures of MAST12 with 8YSZ under similar conditions as described previously. It is interesting to note that the glass MAS by the interaction with 8YSZ gives rise to the formation of cordierite. However, the cordierite phase is not formed by this interaction if the glass MAST5 with 2% of TiO_2 is used. In contrast to this, the cordierite phase is formed in the glass MAST5 after similar heat-treatment as the powder mixture. The cordierite phase is again suppressed in the interaction of 8YSZ with the sealant MAST12 containing 4.9% TiO_2 as nucleating agent. It is known that TiO_2 induces phase separation,

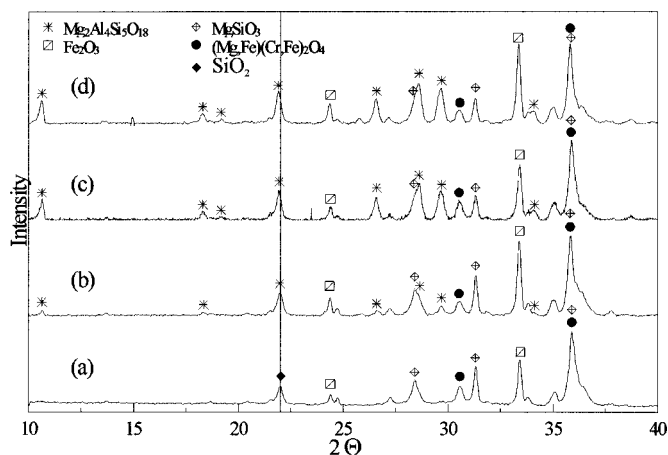


Figure 4. XRD pattern of powder mixtures of (a) MAS + steel, (b) MAST5 + steel, (c) MAS10 + steel, and (d) MAST10 + steel heated at 1000°C for 1000 h.

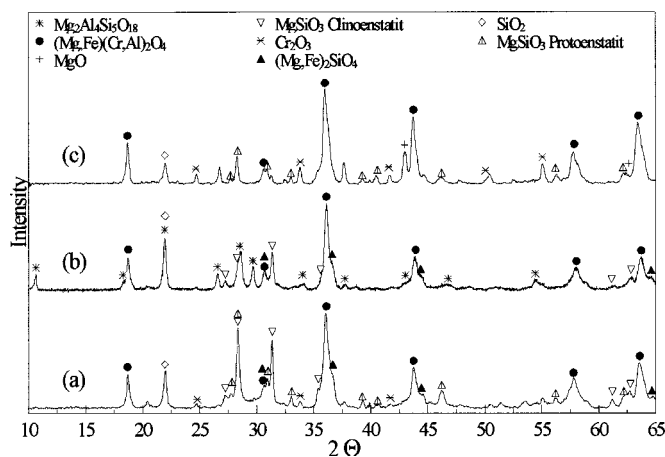


Figure 5. XRD pattern of powder mixtures of (a) MAS + ODS, (b) MAS10 + ODS (100 h), and (c) MAS10 + ODS (500 h) heated at 1000°C .

and possibly Zr ions from 8YSZ diffuse to favor formation of ZrSiO_4 phase in one of the separated regions. The kinetics of this phase formation is probably much faster than the incubation period for the cordierite phase. Phases such as MgSiO_3 and Mg_2SiO_4 get favorably crystallized in the other phase-separated region. MgSiO_3 is the second major phase of the reaction products of 8YSZ and the sealants MAS or MAST5 which contain 0 or 2% TiO_2 , respectively. The Mg_2SiO_4 phase is present in minor amount. If the TiO_2 content is increased to 4.9% (MAST12), the second major product phase is Mg_2SiO_4 . It seems that the content of TiO_2 has a strong influence on the nucleation and crystallization behavior of the glass. Both the nucleation and crystallization temperatures decrease if the TiO_2 content is raised (see Fig. 3). This could change the phase separation phenomena and crystallization kinetics of the glass, resulting in an increase of nuclei of Mg_2SiO_4 as more TiO_2 is used as nucleating agent. According to a report of Ray *et al.*,¹⁰ the increase in nuclei in a glass causes a decrease of T_g and T_c values in DTA. As seen in Fig. 3, the decrease in T_g and T_c with increase in TiO_2 content may refer to the increase of the nuclei of Mg_2SiO_4 which become maximum when the TiO_2 content is 4.9% in sealant MAST12.

Figure 4 shows the XRD pattern of powder mixtures of (a) MAS + steel, (b) MAST5 + steel, (c) MAS10 + steel, and (d) MAST10 + steel heated at 1000°C for 1000 h in air between the 2θ values of 10 and 40° . The diffraction line at about 10.5° , which corresponds to the cordierite phase, and the line at about 21.9° , which may originate from both the cordierite and the cristobalite phase, is considered in the following. The vertical line drawn is a guide for observing minor shift in line position, which may be due to overlapping line positions of cordierite and cristobalite. The intensity ratio of the two lines of cordierite (one at $\sim 10.5^\circ$ and the other at $\sim 21.9^\circ$) can be taken as a guideline to unravel qualitatively the relative volume fractions of the cristobalite and the cordierite phases. From this figure, it is clear that the cordierite phase is not formed in the powder mixture of MAS + steel, but the cristobalite phase can be identified. In contrast to this, the cordierite and the cristobalite phases are formed if the glass MAS was given the same heat-treatment as the mixture. It appears that chromium from the steel acts as an inhibitor for the growth of cordierite in these powder mixtures. The amount of cordierite phase is negligible in the MAST5 + steel mixture. However, for the powder mixtures of sealant MAS10 or MAST10 with steel, the amount of cordierite phase is substantial and possibly the volume fraction of the cristobalite phase is small. There seems to be a competition between the formation of these two phases. Cordierite phase seems to be the favored phase if the alumina content is 10%, as can be expected on the basis of the phase diagram of the $\text{MgO-Al}_2\text{O}_3\text{-SiO}_2$ system. It is possible that

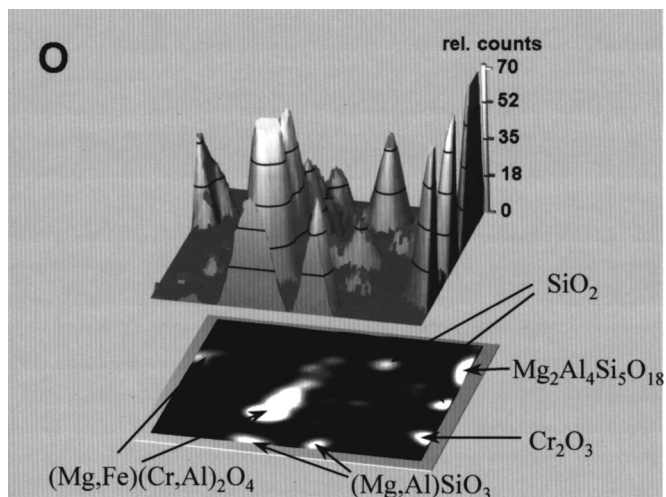


Figure 6. Element mapping analysis of powder mixtures of MAS10 + ODS heated at 1000°C for 500 h by TEM/EDX.

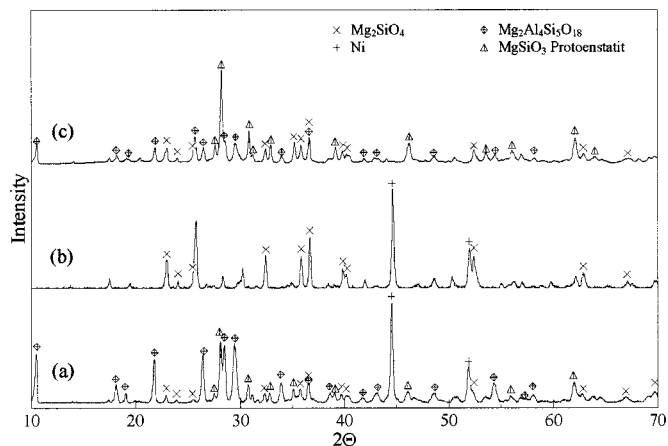
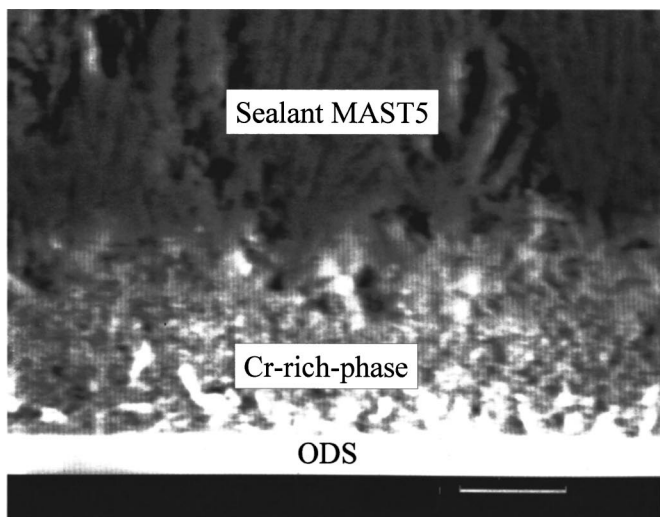
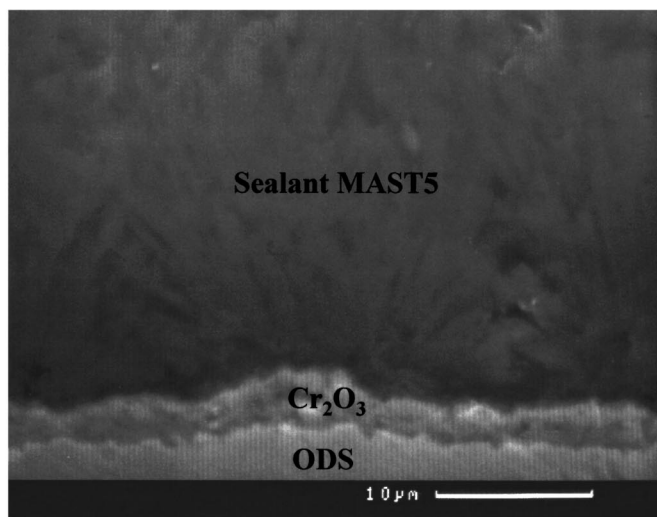


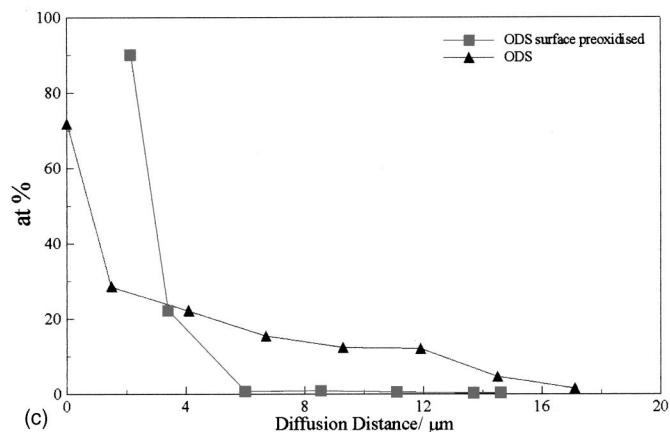
Figure 7. XRD pattern of powder mixtures of (a) MAS10 + Ni, (b) MAS + Ni, and (c) MAS after annealing under reducing conditions at 1000°C for 500 h.



(a)



(b)



(c)

Figure 8. SEM micrographs of interface of MAST5 + ODS (a, top left) without special treatment of the alloy surface before joining, (b, top right) after oxidizing the alloy surface before joining, and (c, left) diffusion profile of chromium in (a) and (b). Both samples were given heat-treatment at 1000°C for 50 h.

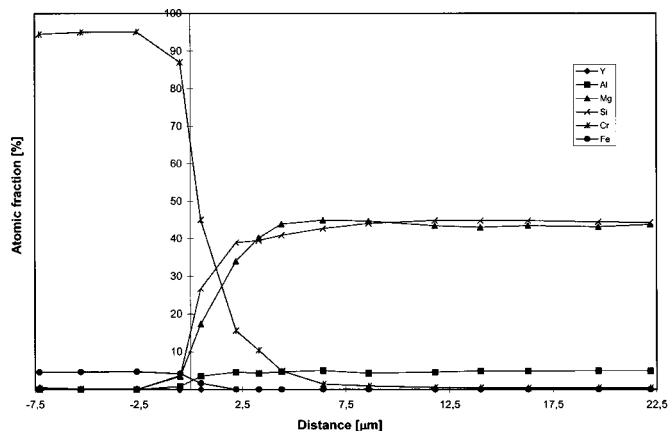
initially the cristobalite phase is favored. However, with longer duration, the cordierite gets nucleated. This conjuncture gets strengthened when we discuss the results of the powder mixtures of the sealants MAS and MAS10 with ODS.

As shown in Table II, one of the reaction products of ODS with most MgO base sealants is a spinel phase whose approximate composition is estimated as $(\text{Mg,Fe})(\text{Cr,Al})_2\text{O}_4$. Besides the spinel phase, the cristobalite phase is also present in many reaction products. In addition, the cordierite phase is present if the Al_2O_3 content of the sealant is 10%. Again, chromium seems to play the role of an inhibitor for the cordierite phase.

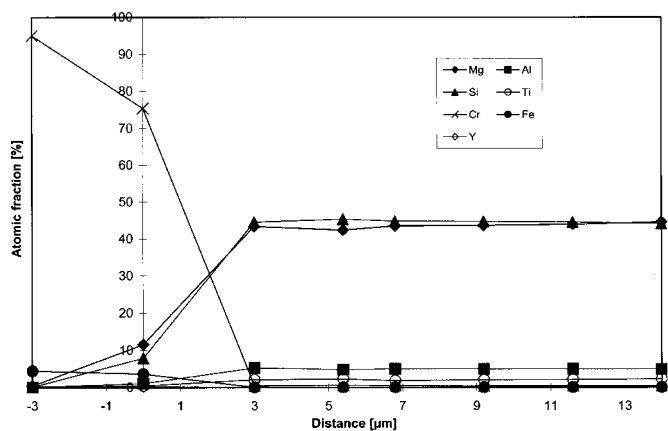
Figure 5 shows the XRD patterns of powder mixtures of (a) MAS + ODS, (b) MAS10 + ODS (500 h), and (c) MAS10 + ODS (100 h) heated at 1000°C . The role of Al_2O_3 content and the competition between cristobalite and cordierite phase formation can also be seen here. If the MAS10 + ODS mixture is heated for 100 h, the cordierite phase is not seen, but the presence of cristobalite is obvious. However, if heated for 500 h, the cordierite phase forms whereas the cristobalite phase is not evident. Similarly, in the powder mixture of MAS + ODS heated at 1000°C for 500 h, the cordierite phase is unable to nucleate although the presence of cristobalite phase is obvious. Kata *et al.*¹¹ and Imanaka *et al.*¹² have shown that cordierite as well as many other aluminum base ceramics can suppress the formation of cristobalite in borosilicate glass and the common factor for this suppression is the Al^{3+} ion. It has also been demonstrated that cristobalite prevention depends on the amount of alumina present in the composite. Jean and Gupta^{13,14} have discussed the suppression of cristobalite in the presence of a small amount of alumina in borosilicate as well as high-silica glasses. The suppression has been attributed to the strong affinity between Al^{3+} and alkali ions forming a K^+ - and Al^{3+} -rich reaction layer more rapidly than the nucleation of cristobalite.¹³ However, this is only possible if the alumina content is above a threshold concentration. It may also be possible for the present set of samples that the content of alumina plays an important role and the competitive formation reaction between cristobalite and cordierite depends upon the content of Al^{3+} as well as temperature and time.

Figure 6 shows the approximate phase distribution of powder mixtures of MAS10 + ODS heated at 1000°C for 500 h on the basis of element mapping by TEM/EDX. The detailed analysis (not included here) shows an affinity between Mg and Cr. The affinity between Mg and Cr ions has also been evidenced by SEM/EDX in the diffusion couples of different sealants with ODS leading to the formation of a spinel phase as discussed in the previous section. Silicon is often found in the reaction zone in which chromium and magnesium are diffused if the interface is annealed for a longer duration. However, silica does not form any phase with chromia. This is also known from the phase diagram of the binary and ternary systems. The phase diagram of Cr_2O_3 - SiO_2 further suggests the formation of cristobalite.

The XRD pattern of powder mixtures of (a) MAS + Ni and (b) MAS10 + Ni heated in reducing atmosphere at 1000°C for 500 h are shown in Fig. 7. Figure 7c shows the XRD pattern of sealant MAS heated under similar conditions as the powder mixtures for comparison. Forsterite (Mg_2SiO_4) formation is shown by all the XRD patterns in Fig. 7. The cordierite phase is formed in pure MAS as well as in the mixture of MAS10 with Ni. It is interesting to note that in the mixture of Ni with MAS, Ni seems to favor the formation of forsterite (Mg_2SiO_4) phase, which presumably suppresses the formation of cordierite in the powder mixture MAS + Ni. As shown in Fig. 7, the cordierite phase is not suppressed if the sealant MAS is given the same heat-treatment as the mixtures. However, the amount of forsterite seems to be small in this material and the amount of MgSiO_3 (protoenstatite) is the highest as compared to that of other product phases formed. This phase is completely absent in the powder mixture of sealant MAS with nickel. It seems that the diffusion of Ni in the glass lattice is helpful in nucleating the forsterite (Mg_2SiO_4) phase which in turn suppresses the formation of



(a)



(b)

Figure 9. Typical diffusion profiles of different cations at the interface of (a, left) MAS + ODS and (b, right) MAST5 + ODS annealed at 900°C for 380 and 12 h, respectively.

cordierite when the alumina content is low (5%). It has been demonstrated that nickel promotes the forsterite formation in the $\text{MgO-CaO-Al}_2\text{O}_3\text{-SiO}_2$ glass system.¹⁵ Nickel in the ionic state can substitute for the Mg^{2+} ion in the octahedral site of the forsterite structure. Comparing the XRD pattern of MAS and MAS + Ni powder mixtures, it is pertinent that Ni induces the formation of forsterite phase in the powder mixture of MAS + Ni rapidly enough so as to suppress the formation of cordierite. This is not the case for the pure sealant MAS in which the favored phase is MgSiO_3 (protoenstatite).

Interdiffusion at the sealant/interconnect interface.—Figure 8 shows the SEM micrographs of the interface of MAST5 + ODS (a) without special treatment of the alloy surface before joining, (b) after oxidizing the alloy surface before joining, and (c) the diffusion profile of chromium in (a) and (b). The two samples were heat-treated at 1000°C for 50 h. The interface made after oxidation of the alloy shows a better adhesion, and the reaction at the interface is significantly less as compared to the interface made without preoxidation. The advantage of preoxidation has also been described earlier in the literature.¹⁶⁻¹⁸ Oxygen plays an important role in promoting strong bonds between metal and oxide ceramics. Oxygen as a surface active agent lowers the surface tension of the metal, enhancing the spreading of the liquid, which leads to better adhesion. It has been shown by Jiang and Silcox¹⁹ that the formation of a graded chromium oxide layer at the interface yields good adhesion. Jiang and Silcox¹⁹ have carried out a detailed investigation by electron

Table III. Diffusion coefficient data for chromium in different sealants determined from the diffusion across the interface of selected sealants with the ODS alloy under different conditions of annealing.

Sealant	Kind of glass	Heat-treatment	Diffusion coefficient (cm ² s ⁻¹)
MAS	5% Al ₂ O ₃	900°C/380 h	2.0×10 ⁻¹⁴
MAS10	10% Al ₂ O ₃	780°C/3 h + 900°C/500 h	1.56×10 ⁻¹⁴
MAST10	10% Al ₂ O ₃ , 2% TiO ₂	780°C/3 h + 900°C/500 h	1.56×10 ⁻¹⁴
MAST5	5% Al ₂ O ₃ , 2% TiO ₂	780°C/3 h + 900°C/500 h	3.1×10 ⁻¹³
MAST5	5% Al ₂ O ₃ , 2% TiO ₂	900°C/12 h	1.56×10 ⁻¹⁴
MAST5	5% Al ₂ O ₃ , 2% TiO ₂	900°C/50 h	3.5×10 ⁻¹⁴
MAST5	5% Al ₂ O ₃ , 2% TiO ₂	900°C/100 h	2.4×10 ⁻¹⁴
MAST5	5% Al ₂ O ₃ , 2% TiO ₂	1000°C/24 h	1.1×10 ⁻¹²
MAST5	5% Al ₂ O ₃ , 2% TiO ₂	1000°C/50 h	1.2×10 ⁻¹²

energy loss spectroscopy (EELS) at the interfaces of chromium/alkaline earth boroaluminosilicate glasses. An important observation of their EELS studies is that the initial oxidized layer consists of Cr²⁺ ions, which possess high oxygen affinity, and is therefore considered to be chemically very active. If such a preoxidized layer is joined with the magnesium aluminosilicate glass, there is a strong tendency of the Cr²⁺ ion to go to higher valence states than 2+. The magnesium ion being a modifier ion has relatively high mobility. Driven by the difference in the heats of oxide formation, ion exchange between Cr²⁺ and Mg²⁺ could occur, giving rise to metallic magnesium and higher oxidation states of chromium. The close affinity between magnesium and chromium ions has already been demonstrated by our SEM/EDX and TEM/EDX studies (cf. previous section). Therefore, it is expected that magnesium will segregate at the interface, having two effects: (i) the magnesium-rich layer will form a barrier layer for the diffusion of chromium and (ii) the [SiO₄]⁴⁻ tetrahedral network will be severely distorted, thereby further reducing the open structure and increasing the viscosity of the sealant inhibiting diffusion of chromium.

Figure 9 shows typical diffusion profiles of different cations at the interface of (a) MAS + ODS, and (b) MAST5 + ODS annealed at 900°C for 380 and 12 h, respectively. The two diffusion profiles exhibit essentially similar features. The main diffusing ions are chromium from ODS as well as Mg from the sealant. These elements are present in significant amounts within the reaction layer. This is in agreement with the formation of spinel phase in the reaction layer containing magnesium and chromium ions, subsequently suppressing the formation of cordierite. However, cristobalite, another detrimental phase, is formed instead (see Table II).

From the diffusion profile of chromium across the interface of ODS with different sealants, the diffusion coefficient was estimated. The results are presented as relative atomic fraction vs. distance into the reaction layer from the ODS to the glass side. The concentration of Cr decreases from the ODS surface into the diffusion layer with respect to time. The concentration of Mg decreases from sealant to the ODS side. From the diffusion profile of the diffusing cations the diffusion coefficient is evaluated by using the following relation

$$\frac{c(x,t)}{c_0} = 1 - \operatorname{erf}\left[\frac{x}{2\sqrt{Dt}}\right] \quad [1]$$

where $c(x,t)$ is the concentration of ions at the distance, x , from the surface of Cr₅Fe₁Y₂O₃ for a given diffusion time period, t . The term c_0 is the initial concentration of ions and D the diffusion coefficient. The term erf stands for error function and its values vary from 0 to 1 for varying values of $x^2/4Dt$ between 0 and 3. The diffusion coefficient of Cr in the sealants of the diffusion couples are summarized in Table III.

Some of the noteworthy features are

1. Diffusion couples of different sealants given the same heat-treatment yield essentially similar values for the diffusion coefficients.

2. If the time of heat-treatment at a fixed temperature for a particular sample is varied, it was observed that the diffusion coefficient decreases with increasing time for the heat-treatment (cf. results for sealant MAST5). This can be explained by the crystallization of the glass which restricts the movement of ions.

3. If the temperature of heat-treatment is varied but the duration was kept fixed (cf. results of sealant MAST5 at 900°C over 50 h and at 1000°C over 50 h), the diffusion coefficient is high for high temperatures as expected.

4. For the interface of MAST5 + ODS, with a preoxidized surface of ODS, the diffusion coefficient amounts to 8×10^{-14} cm² s⁻¹ (not shown in Table III), which is much less compared to the value without preoxidation, which amounts to 1.2×10^{-12} cm² s⁻¹. Both the samples were given the same heat-treatment (1000°C for 50 h). This aspect is also reflected by Fig. 8 as discussed previously. Thus, the diffusion of chromium can be reduced substantially by preoxidizing the surface of ODS before making the interface.

Conclusion

The chemical interactions between different aluminosilicate base glass sealants and components on the anode side of SOFCs have been investigated. The sealants with BaO and CaO as network modifiers are not found suitable due to extensive crystallization and reaction at the interfaces. MgO base glasses, which have been studied in more detail with varying alumina content or with TiO₂ as nucleating agent, offer better possibilities. The formation of detrimental phases such as cordierite and cristobalite was observed in different powder mixtures and diffusion couples. We have made an attempt to get insight into the conditions under which these phases are formed. The implication of these investigations is that the formation of these phases can be avoided by suitably choosing the composition and the nucleating agent. The interdiffusion investigations reveal that the diffusion of chromium is maximum across the interfaces of sealant/interconnect. A rough estimate suggests that chromium may diffuse up to 0.9 mm in a time period of 50,000 h if operated at 1000°C, which is considered the lifetime of SOFCs.

The Institute for Materials and Processing in Energy Systems, Forschungszentrum Jülich GmbH, assisted in meeting the publication costs of this article.

References

1. K. L. Ley, M. Krumpelt, R. Kumar, J. H. Meisser, and I. Bloom, *J. Mater. Res.*, **11**, 1489 (1996).
2. S. V. Phillips, A. K. Dutta, and L. Lakin, in *Proceedings of the 2nd International Symposium on Solid Oxide Fuel Cells*, F. Grosz, P. Zegers, S. C. Singhal, and O. Yamamoto, Editors p. 737, Commission of the European Communities, Report E4R 13456EN, Athens, Greece (1991).
3. Y. M. Sung, *J. Mater. Sci.*, **31**, 5421 (1996).
4. Y. Sakaki, M. Hattori, and Y. Esaki, in *Solid Oxide Fuel Cells V*, U. Stimming, S. C. Singhal, H. Tagawa, and W. Lehnert, Editors, PV 97-40, The Electrochemical Proceedings Series, p. 652, Pennington, NJ (1997).
5. C. Günther, G. Hofer, and W. Kleinlein, in *Solid Oxide Fuel Cells V*, U. Stimming, S. C. Singhal, H. Tagawa, and W. Lehnert, Editors, PV 97-40, p. 746, The Electrochemical Society Proceedings Series, Pennington, NJ (1997).

6. T. Horita, N. Sakai, and T. Kawada, *Denki Kagaku*, **61**, 760 (1993).
7. N. Lahl, K. Singh, L. Singheiser, K. Hilpert, and D. Bahadur, *J. Mater. Sci.*, **38**, 3089 (2000).
8. N. Lahl, L. Singheiser, K. Hilpert, K. Singh, and D. Bahadur, in *Solid Oxide Fuel Cells VI*, S. C. Singhal and M. Dokiya, Editors, PV 99-19, p. 1057, The Electrochemical Society Proceedings Series, Pennington, NJ (1999).
9. L. Kinderman, D. Das, D. Bahadur, R. Nickel, and K. Hilpert, *J. Am. Ceram. Soc.*, **80**, 909 (1997).
10. C. R. Ray, W. Huang, and D. E. Day, *J. Am. Ceram. Soc.*, **74**, 160 (1991).
11. K. Kata, Y. Shimada, and H. Takamizawa, *IEEE Trans. Compon., Hybrids, Manuf. Technol.*, **CHMT-13**, 448 (1990).
12. Y. Imanaka, A. Shigenori, N. Kamehara, and K. Niwa, *J. Am. Ceram. Soc.*, **78**, 1265 (1995).
13. J. H. Jean and T. K. Gupta, *J. Mater. Res.*, **8**, 2393 (1993).
14. J. H. Jean and T. K. Gupta, *Phys. Chem. Glasses*, **36**, 176 (1995).
15. L. Barbieri, A. M. Ferrari, C. Leonelli, T. Manfredini, G. C. Pellacani, S. Bruni, and F. Cariatti, *Phys. Chem. Glasses*, **36**, 176 (1995).
16. A. Zanchetta, P. Lefort, and E. Gabbay, *J. Eur. Ceram. Soc.*, **15**, 233 (1995).
17. A. A. Zanchetta, P. Lortholary, and P. Lefort, *J. Alloys Compd.*, **228**, 86 (1995).
18. C. Beraud, M. Courbiere, C. Esnouf, D. Juve, and D. Treheux, *J. Mater. Sci.*, **24**, 4545 (1989).
19. N. Jiang and J. Silcox, *J. Appl. Phys.*, **87**, 3768 (2000).